Paraconductivity study in $ErBa_2Cu_{3-x}M_xO_{7-\delta}$ (M = Zn, Fe) superconductors

A. Sedky[a)b)†] and S. B. Mohamed[a)]

[a)] *Physics Department, Faculty of Science, King Faisal University, Al-Hassa* 31982, *Saudi Arabia*
[b)] *Physics Department, Faculty of Science, Assiut University, Assiut, Egypt*

(Received 13 June 2013; revised manuscript received 2 August 2013)

We report here the paraconductivity of $ErBa_2Cu_{3-x}M_xO_{7-\delta}$ (M = Zn and Fe) superconductors. The logarithmic plots of excess conductivity $\Delta\sigma$ and reduced temperature $\mathbb{C}$ reveal two different exponents corresponding to crossover temperature as a result of shifting the order parameter from 2 to 3. The first exponent in the normal field region is close to 1, in which the order parameter dimensionality (OPD) is 2. The second exponent in the critical field region is close to 0.5, in which the OPD is 3. The coherence length, interlayer coupling, interlayer separation and carrier concentration decrease with increasing doping content, and their values for Fe samples are different from those of Zn samples. While anisotropy is increased with increasing doping content, it is generally higher for a Zn sample than that for an Fe sample. We also estimate several physical parameters such as upper critical magnetic fields in the a–b plane and along the c axis (B_{ab} and B_c), and critical current density J at 0 K. Although B_{ab} and B_c are generally increased with doping content increasing, the value of B_{ab} is found to be twice more than that of B_c. A similar behavior is obtained for J (0 K) and its value is higher in the Fe sample than that in the Zn sample. These results are discussed in terms of oxygen deficiency, localization of carriers, and flux pinning, which are produced by doping.

Keywords: ceramics, chemical synthesis, X-ray diffraction, electrical properties, transport properties

PACS: 74.25.Bt, 74.62.Dh, 74.62.En, 74.72.gh **DOI:** 10.1088/1674-1056/22/11/117401

1. Introduction

High temperature superconductors exhibit anisotropy and small coherence length together with elevated values of critical temperature T_c. These parameters have great effects on the thermal fluctuations of superconducting order parameter dimensionality (OPD), which have been observed in the measurements of conductivity versus temperature as excess conductivity.[1] By reducing the temperature from room temperature toward the critical temperature T_c, the fluctuation of Cooper pairs begins to occur spontaneously at a temperature T_f ($T_f = 2T_c$).[2] As the temperature approaches T_c, the number of Cooper pairs increases while the normal electron density decreases. Therefore, the resistivity decreases and the thermal fluctuations induce an excess conductivity $\Delta\sigma$.

The fluctuation induced conductivity (FIC) analyses revealed that the contribution of excess conductivity is due to Gaussian and critical fluctuations in the mean and critical field regions, respectively.[3] Gaussian fluctuation is probably dominant in the temperature region above the mean field temperature T_c^{mf} when the fluctuation in the order parameter is small and the interactions between Cooper pairs can be neglected. While the critical fluctuation occurs in the critical field region close to T_c when the fluctuations in the order parameter are large and the interactions between Cooper pairs is considered The variation of Gaussian FIC with the reduced temperature helps to find the dimensional exponents, coherence lengths and crossover temperatures.[4] The dimensional exponents in high-T_c materials are found to be zero-dimensional (0D), one-dimensional (1D), two-dimensional (2D), and three-dimensional (3D). It is seen that the dimensional crossover takes place between any two regions with different dimensions. The crossover from two dimensions to three dimensions is mainly obtained above T_c at a crossover temperature which is different for different samples. However, the crossover temperature is not unique; rather the dimensional crossover takes place over a temperature region.[5]

However, the possibility of oxygen deficiency in Y:123 superconductors, either in CuO_2 planes or in CuO chains, has interesting phenomena due its influences on the critical temperatures of these materials. It has been reported that the oxygen deficiency influences the FIC in most of high T_c superconductors.[6–9] The fluctuation analyses based on Y:123 samples have revealed that there is a crossover from three dimensions to quasi two dimensions by removing the oxygen from CuO chains. A 3D behavior is expected close to T_c when the c-axis coherence length becomes greater than the interlayer spacing.[6,7] While the crossover from three dimensions to two dimensions has been obtained by the created vacancies of oxygen induced by irradiation in the Cu–O_2 planes of Bi: 2212 system.[8,9] In the above background, we report here the order parameter dimensionality response to the oxygen deficiency created by both Zn and Fe doped Er: 123 superconductors.

†Corresponding author. E-mail: sedky1960@yahoo.com; asedky@kfu.edu.sa

© 2013 Chinese Physical Society and IOP Publishing Ltd

2. Experimental details

A series of the samples, $ErBa_2Cu_{3-x}M_x\ O_{7-\delta}$ (M = Zn and Fe) with various x ($0.00 \le x \le 0.18$) is synthesized by using the well-known solid state reaction method. The ingredients Y_2O_3 , $BaCO_3$, CuO, ZnO, and Fe_2O_3 of 4 N purity are thoroughly mixed in required proportions and calcined at 900 °C in air for 16 h, and then the furnace is slowly cooled down to room temperature. This exercise is repeated three times with intermediate grinding at each stage. The resulting powders are ground, palletized into pellets and sintered in at 940 °C for 24 h. Finally, the furnace is cooled down to room temperature with an intervening annealing for 24 h at 600 °C. After that, the samples are characterized for phase purity and oxygen deficiency by X-ray diffraction (XRD) and idometric titration, respectively. The electrical resistivity of the sample is obtained using the standard four-probe technique in a closed cycle refrigerator (cryomech compressor package with cryostat Model 810-1812212, USA) within the range of 10–300 K. Nanovoltameter Keithley 2182, current source Keithley 6220, and temperature controller 9700 (0.001 K resolution) are used during these measurements.

3. Results and discussion

The excess conductivity $\Delta\sigma$ due to thermal fluctuation is defined as the deviation of the measured conductivity of $\sigma_m(T)$ from the normal conductivity $\sigma_n(T)$, and expressed as follows:

$$\Delta\sigma = \left(\frac{1}{\rho_m} - \frac{1}{\rho_n}\right) = \sigma_m - \sigma_n, \tag{1}$$

where ρ_m and ρ_n are the measured and normal resistivity, respectively. Normally, ρ_n is obtained from the measured resistivity ρ_m at $T \ge 2T_c$ by applying the least square method to the Anderson and Zou relation, $\rho_n(T) = A + BT$.[10] In order to estimate the paraconductivity, Aslamazov and Larkin (AL)[11] deduced the following relation for the fluctuation- induced excess conductivity $\Delta\sigma$ as

$$\Delta\sigma = A\mathbb{C}^{-\lambda}. \tag{2}$$

Here, $A = e^2/(32\hbar\xi_c(0))$ and $\lambda = 0.5$ for 3D conductivity , and $A = e^2/(16\hbar d)$ and $\lambda = 1.0$ for 2D conductivity, e is the electronic charge, d is the interlayer spacing between two successive CuO_2 planes, $\hbar$ is the reduced Plank constant, $\xi_c(0)$ is the c-axis 3D coherence length at zero temperature, and $\mathbb{C}$ is the reduced temperature given by[10–12]

$$\mathbb{C} = \frac{T - T_c^{mf}}{T_c^{mf}}, \tag{3}$$

where T_c^{mf} is the mean field temperature, above which the interactions between Cooper pairs can be neglected. The plot of

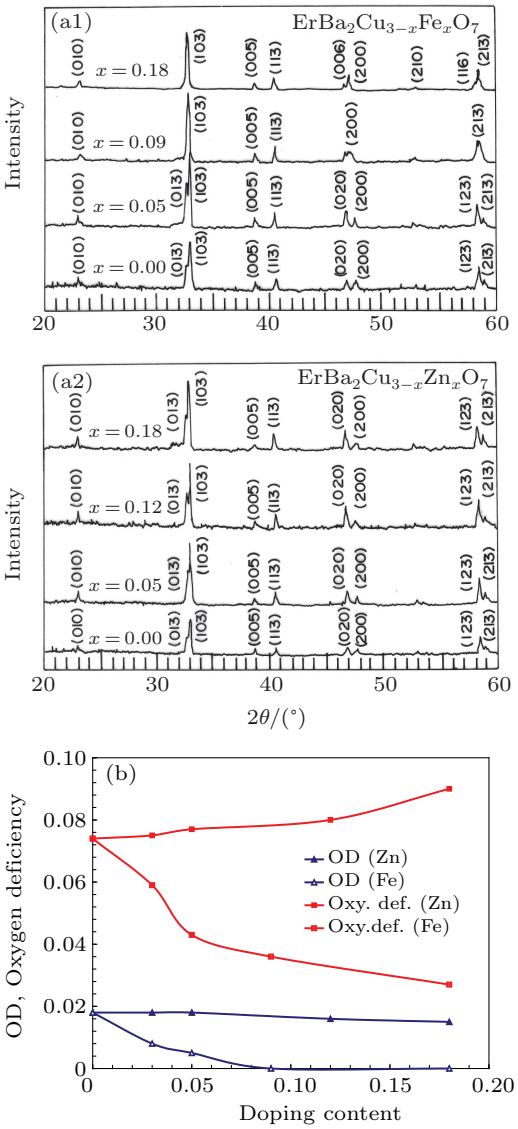


Fig. 1. (color online) (a) X-ray diffraction patterns for $ErBa_2Cu_{3-x}M_xO_{7-\delta}$ samples, and (b) curves of orthorhombic distortion and oxygen deficiency versus doping content for $ErBa_2Cu_{3-x}M_xO_{7-\delta}$ samples.

$d\rho/dT$ versus T is made for obtaining the value of T_c^{mf} from the peak. However, for the polycrystalline sample, the modified equations for 2D and 3D fluctuations are expressed as[13]

$$\Delta\sigma_{3D} = \frac{e^2}{32\hbar\xi_p(0)}\varepsilon^{-\frac{1}{2}}, \tag{4a}$$

$$\Delta\sigma_{2D} = \frac{1}{4}\left\{\frac{e^2}{16\hbar d}\varepsilon^{-1}\left[1 + \left(1 + \frac{8\xi_c^4(0)}{d^2\xi_{ab}^2(0)}\varepsilon^{-1}\right)^{\frac{1}{2}}\right]\right\}, \tag{4b}$$

where $\xi_{ab}(0)$ is the coherence length at 0 K across the ab plane and $\xi_p(0)$ is the effective characteristic coherence length at 0 K.

On the other hand, the cross over behavior from two dimensions to three dimensions occurs at a temperature T_0 given by[12]

$$T_0 = T_c^{mf}\exp\left(\frac{2\xi_c(0)}{d}\right)^2, \tag{5}$$

where $\xi_c(0)$ is given by[14,15]

$$\xi_c(0) = \left(\frac{dk^{1/2}}{2}\right), \tag{6}$$

with k being the interlayer coupling and expressed by[16]

$$k = \ln\left(\frac{T_0}{2T_c^{mf}}\right). \tag{7}$$

Figure 1(a) shows the XRD patterns of pure and doped samples. It is clear that the Zn samples are clearly orthorhombic, which is evident from crystallographic splittings of (020), (200) and (123), (213). The Fe samples with $x = 0.03$ and 0.05 are orthorhombic, while the samples with $x = 0.09$ and 0.18 are tetragonal. Figure 1(b) shows the orthorhombic distortion (OD) and oxygen deficiency versus doping content. Similar values are listed in Table 1. The values of OD vary from 0.018 for pure sample to 0.017 for Zn samples, and to 0.00 for Fe samples. The values of oxygen deficiency vary from 0.074 for pure sample up to 0.090 for the Zn samples and to 0.059 for the Fe samples.

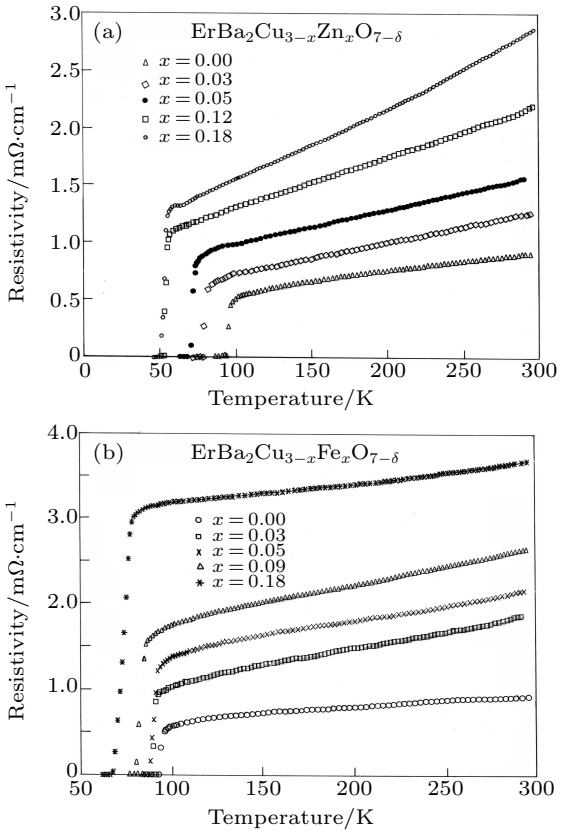


Fig. 2. Curves of resistivity versus temperature for (a) $ErBa_2Cu_{3-x}Zn_xO_{7-\delta}$ samples, and (b) $ErBa_2Cu_{3-x}Fe_xO_{7-\delta}$ samples.

The curves of resistivity versus temperature for pure and doped samples are given in Figs. 2(a) and 2(b). It is found that the normal resistivity is linear as temperature decreases from room temperature down to a certain temperature T_B. In this region, $\rho_n(T)$ follows the above formula, $\rho_n(T) = A + BT$ as discussed above. $T_B = 2T_c^{mf}$, and is defined as the temperature below which the Cooper-pair formation starts.[17] As the temperature further decreases beyond the normal state region, the decreasing rate of resistivity becomes entirely different as compared with that in this region. This is mainly due to increasing Cooper pair formation with decreasing temperature. Therefore, the FIC in this region follows the A–L model to yield the dimensional exponent appropriate to fluctuation-induced conductivity in these samples.

The normal resistivity $\rho_n(T)$ is calculated in terms of A and B parameters which are obtained from the linear fitting of the measured resistivity. The values of mean field temperature T_c^{mf} for all samples are estimated from the plot of peak of $d\rho/dT$ against temperature as shown in Figs. 3(a) and 3(b). After that we calculate the excess conductivity $\Delta\sigma$ and reduced temperature $\mathbb{C}$ as discussed above. We plot the curves of $\ln\Delta\sigma$ against $\ln\mathbb{C}$ for all samples, see Figs. 4(a) and 4(b). It is evident from the fitting that there is distinct change in the slope of each plot. The corresponding temperature where the slope change occurs is designated to the crossover temperature T_o. Figure 5(a) shows the variations of T_c , T_o, and T_c^{mf} against doping content. Similar values are listed in Table 1. It is clear that both T_c and T_c^{mf} decrease with increasing doping content, and their values are generally higher for Fe samples than those for Zn samples. However, T_o decreases for Zn sample and for Fe, T_o increases up to 0.0.09, then decreases with doping content further increasing up to 0.18.

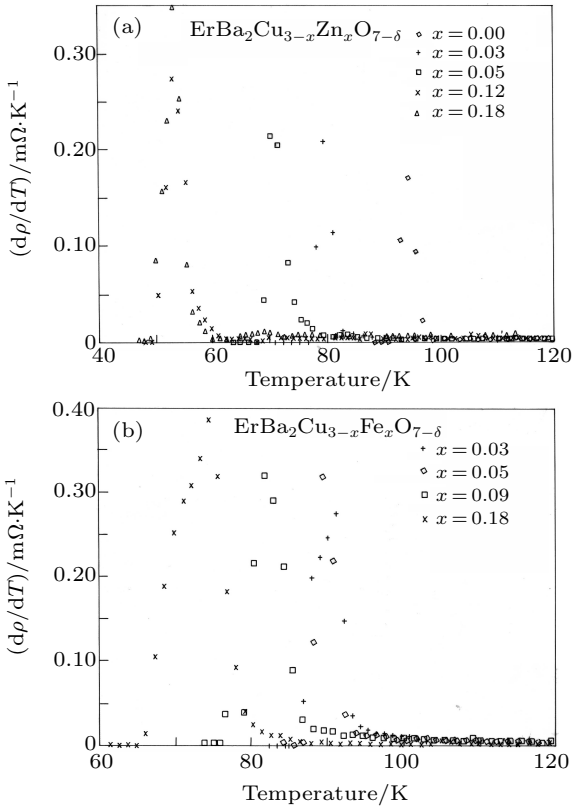


Fig. 3. Curves of $d\rho/dT$ versus temperature for (a) $ErBa_2Cu_{3-x}Zn_xO_{7-\delta}$ samples and (b) $ErBa_2Cu_{3-x}Fe_xO_{7-\delta}$ samples.

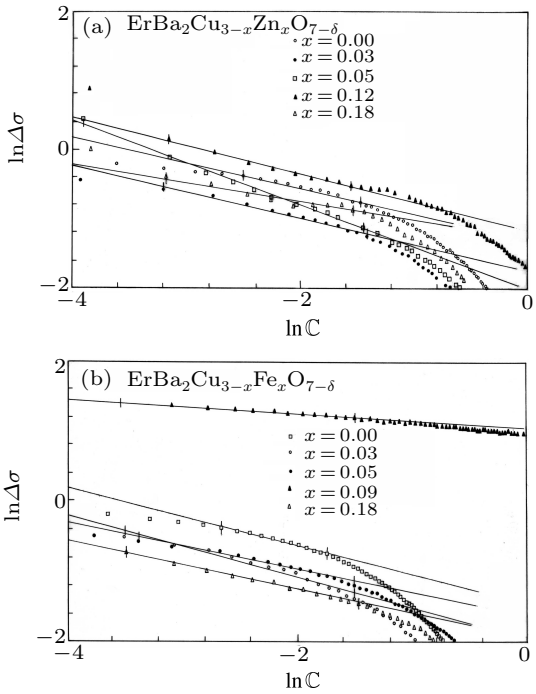


Fig. 4. Curves of $\ln\Delta\sigma$ against $\ln\mathbb{C}$ for (a)$ErBa_2Cu_{3-x}Zn_xO_{7-\delta}$ samples and (b) $ErBa_2Cu_{3-x}Fe_xO_{7-\delta}$ samples.

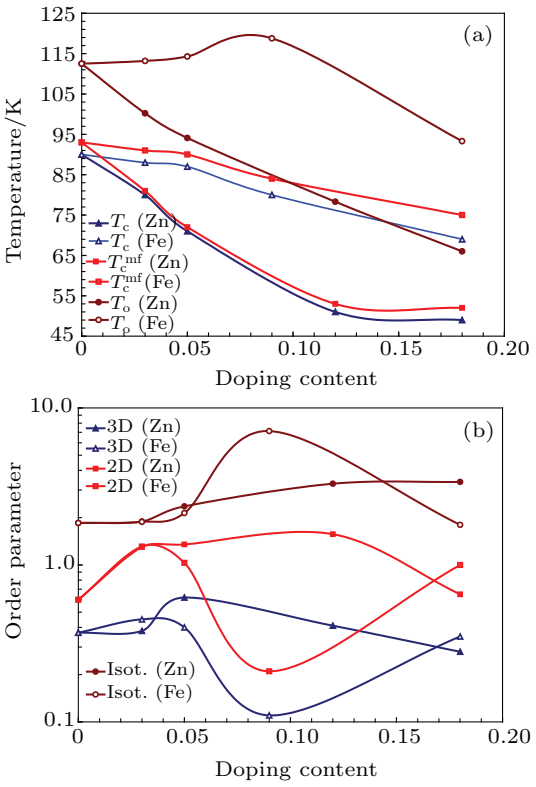


Fig. 5. (color online) Curves of (a) T_c, T_c^{mf} and T_o and (b) hole carrier and interlayer coupling versus doping content for $ErBa_2Cu_{3-x}M_xO_{7-\delta}$ samples.

However, two different exponents corresponding to the crossover temperature are obtained from each plot with an accuracy of ±1 K. The first exponent occurs at $(0.00 \geq \ln\mathbb{C} \geq -1.2)$ for Zn samples, and at $(-0.60 \geq \ln\mathbb{C} \geq -1.5)$ for Fe samples, and its values are higher than 1, in which the OPD is 2.[18] The second exponent occurs at $(-1.2 \geq \ln\mathbb{C} \geq -4)$ for Zn samples, and at $(-1.5 \geq \ln\mathbb{C} \geq -4)$ for Fe samples, and its values are close to 0.5, in which the OPD is 3. Figure 5(b) shows the variations of OPD versus doping content for all samples. Similar values are listed in Table 1. These results reveal that the OPD is shifted from 2 to 3 as temperature decreases towards T_c. However, more than one region has been reported in each of pure and doped Y:123 samples.[19,20] Normally, the critical field region is controlled by the critical fluctuation resulting from the small mean free path of the charge carriers and also due to short coherence length produced as the carrier concentration is changed.[20–23] Anyhow, the dimensional nature in RE:123 system is supposed to be 3D conduction. But in some recent studies based on Y:123 superconductors, the presence of 2D fluctuation conduction is certified. Furthermore, an intermediate crossover region between two dimensions and three dimensions is reported, which is consistent with the results in the present work.[24–26]

On the other hand, Presland *et al.*[27] have found that the phase diagrams for pure and doped high T_c systems, and they are described by the following parabolic formula:

$$\frac{T_c^m}{T_c^x} = 1 - 82.6(p - 0.16)^2, \tag{8}$$

where T_c^x and T_c^m are the critical and maximum critical temperature, respectively and p is the hole carrier concentration per Cu ion and calculated using the above parabolic relationship. Figure 6(a) shows the variations of k and p against doping content. Similar values are listed in Tables 1 and 2. It is found that the values of k and p decrease with doping content increasing up to 0.12 then increase with doping content further increasing up to 0.18, and their values are slightly higher for Fe samples than those of Zn samples. Anyhow, a universal dome-shaped curve of T_c versus carrier concentration has been observed in Y:123 system.[28] It is has been also reported that T_c increases with increasing carrier concentration until it passes through a maximum, after which it decreases and becomes zero above an optimum value of concentration.[28] Actually, the Y:123 system is essentially 3D with two CuO_2 planes and one CuO chain which manifests in the higher values of k and lower degree of anisotropy γ.[29] However, the decrease in k with doping content increasing suggests that the system may become more highly anisotropic, and consequently the charge carriers are either increased or localized. However, anisotropy values will be presented in the next paragraph.

For polycrystalline samples, $\xi_p(0)$ is given by[13]

$$\frac{1}{\xi_p(0)} = \frac{1}{4}\left[\frac{1}{\xi_c(0)} + \left(\frac{1}{\xi_c^2(0)} + \frac{8}{\xi_{ab}^2(0)}\right)^{\frac{1}{2}}\right]. \tag{9}$$

Also, T_0 is related to the crossover temperature as follows:

$$T_0 = T_c\left\{1 + \frac{\xi_p^2(0)}{d^2}\left[1 + \frac{\xi_p^2(0)}{16\xi_{ab}^2(0)}\right]\right\}. \tag{10}$$

Therefore, $\xi_{ab}(0)$ and d are calculated in terms of T_0, T_c , $\xi_p(0)$, and $\xi_c(0)$ values. Then, anisotropy parameter $\gamma = \xi_{ab}(0)/[\xi_c(0)]$ are easily obtained. Figure 6(b) shows the behaviors of $\xi_c(0)$, $\xi_{ab}(0)$, $\xi_p(0)$, and d parameters against doping content Also, anisotropy parameter γ against doping content is enclosed with OPD in Fig. (5b). Similar values are listed in Table 2. It is found that the coherence lengths are generally lower for the doped samples. While, γ increases with increasing doping content and generally higher in the Zn samples than in the Fe samples.

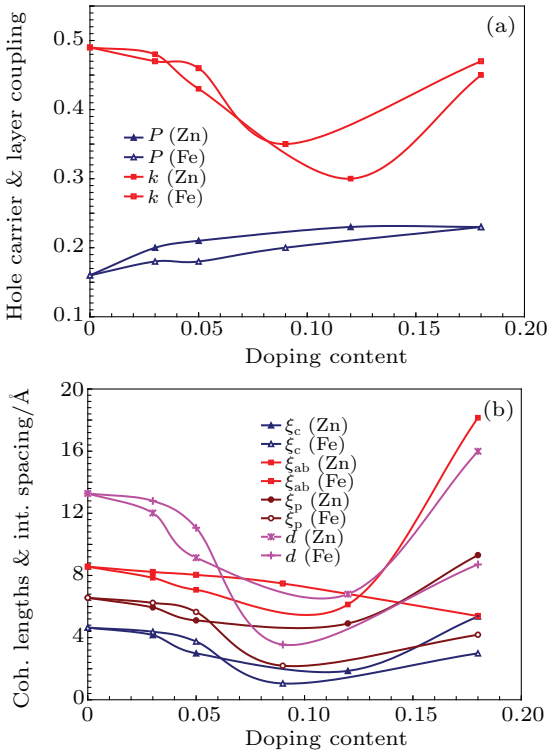


Fig. 6. (color online) Curves of (a) order parameter and anisotropy and (b) coherence length and interlayer spacing versus doping content for $ErBa_2Cu_{3-x}M_x O_{7-\delta}$ samples.

The upper critical fields along the c axis and a–b plane, and critical current density at 0 K. J (0 K) are estimated by the following relations:[30,31]

$$B_{II}(c) = \frac{\phi_0}{2\pi\xi_{ab}^2(0)}, \quad B_{II}(ab) = \frac{\phi_0}{2\pi\xi_c(0)\xi_{ab}(0)}, \quad (11)$$

$$J_c(0) = \frac{2\phi_0}{\sqrt{6}\pi\mu^2(0)\xi_p(0)}, \quad (12)$$

where ϕ_0 is the quantum flux given by $\phi_0 = h/(2e) = 2.07 \times 10^{-15}(\text{web/m}^2)$, and μ is the London penetration depth at 0 K which is about 150 nm for Y:123 superconductors.[32] However, the behaviors of B against doping content are shown in Fig. (7a), and similar values are listed in Table 2. It is clear that B_{ab} is twice B_c, and their values are different in the Zn and the Fe samples according to the doping region (under doping region/higher doping region). While, critical current density J (0 K) shown in Fig. (7b) generally increases with doping content increasing, and their values are slightly higher in the Fe samples than in the Zn samples. This is due to the enhancement of flux pinning, which may be ascribed to the increase of the pinning centers in these types of samples.[33]

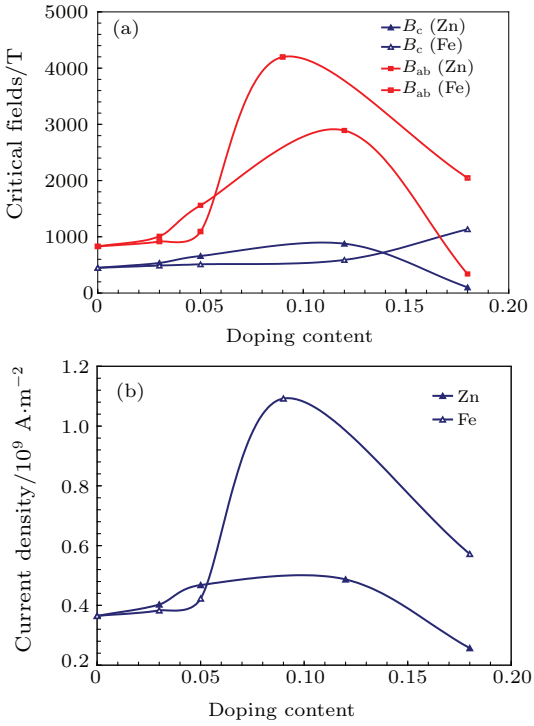


Fig. 7. (color online) Curves of (a) critical magnetic field and (b) critical current density versus doping content for $ErBa_2Cu_{3-x}M_xO_{7-\delta}$ samples.

Table 1. Values of OD, c, oxygen deficiency δ , T_c , T_B, T_c^{mf}, T, λ_{3D}, λ_{2D}, and p for $ErBa_2Cu_{3-x}M_xO_{7-\delta}$ samples with various M and x.

	x	OD	c/Å	δ	T_c/°K	T_B/°K	T_c^{mf}/°K	T_o/°K	λ (3D)	λ (2D)	P
Zn	0.00	0.018	11.684	0.074	90	183	93	112.5	0.37	0.60	0.16
	0.03	0.018	11.683	0.075	80	159	81	100.2	0.38	1.30	0.20
	0.05	0.018	11.683	0.077	71	147	72	94.1	0.62	1.35	0.21
	0.12	0.016	11.683	0.080	51	125	53	78.3	0.41	1.57	0.23
	0.18	0.015	11.690	0.090	49	126	52	66	0.28	0.65	0.23
Fe	0.00	0.018	11.684	0.074	90	183	93	112.5	0.37	0.60	0.16
	0.03	0.008	11.684	0.059	88	181	91	113.2	0.45	1.31	0.18
	0.05	0.005	11.681	0.043	87	179	90	114.3	0.40	1.03	0.18
	0.09	0.000	11.682	0.036	80	171	84	118.8	0.11	0.21	0.20
	0.18	0.000	11.681	0.027	69	161	75	93.3	0.35	1.00	0.23

Table 2. Values of k, $\xi_c(0)$, $\xi_{ab}(0)$, γ, d, $\xi_p(0)$, B_{IIC}, B_{IIab}, and $J(0)$ for $ErBa_2Cu_{3-x}M_xO_{7-\delta}$ samples with various values of M and x.

	x	k	$\xi_c(0)$/Å	$\xi_{ab}(0)$/Å	γ	d/Å	$\xi_p(0)$/Å	B_{IIC}/T	B_{IIab}/T	J/A·m^{-2}
Zn	0.00	0.49	4.64	8.57	1.85	13.28	6.56	448.8	828.9	3.65×10^8
	0.03	0.48	4.16	7.85	1.89	12.02	5.94	534.9	1009.4	4.03×10^8
	0.05	0.43	2.99	7.07	2.36	9.14	5.31	659.4	1559.3	4.68×10^8
	0.12	0.30	1.86	6.13	3.29	6.80	4.91	877.2	2890.9	4.87×10^8
	0.18	0.45	5.36	18.15	3.38	15.99	9.31	100.1	338.8	2.57×10^8
Fe	0.00	0.49	4.64	8.57	1.85	13.28	6.56	448.8	828.9	3.65×10^8
	0.03	0.47	4.38	8.22	1.88	12.80	6.24	487.8	915.5	3.83×10^8
	0.05	0.46	3.75	8.04	2.14	11.07	5.65	510.0	1093.3	4.23×10^8
	0.09	0.35	1.05	7.48	7.12	3.55	2.19	589.1	4196.8	10.9×10^8
	0.18	0.47	2.99	5.39	1.80	8.71	4.18	1134.6	2045.3	5.72×10^8

However, the effects of partial substitution for Cu sites with 3d elements on the properties of Y:123 systems have been extensively investigated. Great attention is focused on the Fe doping owing to the co-existence of magnetic ordering by Fe sublattice and superconductivity.[33–35] It is found that Fe atom attracts additional oxygen atoms and consequently its coordination number is increased. A slight change of superconducting transition temperature T_c is observed for the lower values of Fe content (≤ 0.05). But the further increase of Fe content leads to the abrupt decrease of T_c, and the structure change from orthorhombic to tetragonal phase occurs, which is in agreement with the present data. Furthermore, the pinning force density is increased by 0.09 Fe addition followed by a decrease with the further increase of Fe up to 0.18, which is consistnt with the behaviors of critical fields and critical currents.

A great reduction in the OPD of the Fe samples near the critical field region is observed, which suggests an anomalous crossover as result of much slower supression of superconductivity in the Fe samples than in the Zn samples. An indication, i.e., an OPD of 2 near T_c suggests a deterioration in the CuO_2 coupling in this region. An OPD of 3 in the mean field region and crossover behavior suggest a partial suppresion of fluctuation by Fe. Therefore, the chain site occupancy does not suppress the fluctuation sufficiently fast, owing to the trivalence of Fe. The decrease of oxygen deficiency by Fe cause a decrease in c axis coherence length, thereby resulting in a reduction of mean free path. Therefore, the coupling between CuO_2 planes is not affected drastically, which is in agreement with the value of k. Therefore, the change of OPD with Fe is due to the changing of the superconducting volume fraction, which is in agreement with the reported data.[36,37]

The Zn samples look more 3D near the mean field region in the higher and lower temperature limits. In the critical field region, we observed a dominant parameter with an OPD of 2. In Y:123 system, $\Delta\sigma$ increases by increasing oxygen deficiency δ, which should decouple the CuO_2 planes and increase in the c-axis coherence length. Since δ is invariant by Zn (≈ 0.07), we do not expect decoupling of the CuO chains or an increase in the value of ξ_c or c-axis length, which causes an increase in $\Delta\sigma$.[38] Hence, the behavior of Zn sample is similar to that of the pure sample and the planes remain coupled so strongly. The specific behavior of resistivity of the Zn doped sample for $x = 0.18$ causes the sharp reversal of dimensionality with its exponent approximating to 0.27. The overall OPD behavior, however, is similar to that of low concentration Zn doped sample.

Because of matching ionic radii and divalent oxidation states, substitution of Zn for Cu in Er123 is unlikely to have any significant effect on the carrier density. Cu and Zn have similar valence states, and the charge balance within the CuO_2 plane is not affected. But Zn disorders and disturbs the hybridization and alignment between Cu-3d and O-2p, thereby causing carrier localization in CuO_2 planar networks. The YBCO films and magnetically aligned powders show a strong $\lambda(0)$ increase with the increase of Zn doping content. In London criteria, $n_s(0) \propto \lambda^{-2}(0)$, the $\lambda(0)$ increase corresponds to a large decrease in carrier density n_s.[38–41] Thus, Zn causes a decrease in n_s. The invariant OPD suggests its independence of n_s variation with Zn concentration. The OD is independent of Zn concentration, which indicates an intact oxygen ordering or the linear chain structure. Since Zn does not change the lattice parameters we expect a change neither in the overlap between the Cu-3d and O-2p orbital's nor in the separation between the CuO_2 planes. The nature of the OPD with 3 and its invariance with Zn concentration indicate that the two planes in the unit cell are so coupled that their contributions appear to be due to a single plane.

4. Conclusions

A comparative study between effects of Zn and Fe doping on paraconductivity of Er:123 superconductor is reported. The results show the independence of carrier concentration variation in the CuO_2 planes, and suggest the strong couplings between them for pure and doped samples. For low Fe content, the OPD is invariant and for higher Fe content the OPD shows marked dimensionality variation and increased oxygen content dependence. However, the OPD promotes a dimensionality reversal at 0.18. While OPD remains almost invariant with

respect to Zn doping content, and seems to cause the suppression of 2D fluctuations. The critical field increases with doping content increasing, and then decreases with doping content further increasing up to 0.18, and the values of critical fields are different between Zn and Fe samples. While J (0 K) generally increases with doping content increasing, and the value is slightly higher in the Fe samples than in the Zn samples. This is attributed to the enhancement of flux pinning, which may be ascribed to the increase of the pinning centers produced by Fe in these samples.

References

[1] Fisher D S, Fisher M PA and Huse D A 1991 *Phys. Rev. B* **43** 130
[2] Aswal D K, Singh A, Sen S, Kaur M, Viswandham C S, Goswami G L and Gupta S K 2002 *J. Phys. Chem. Solids* **63** 1797
[3] Maki K and Thompson R S 1988 *Phys. Rev. B* **39** 2767
[4] Vidal F, Veira J A, Maja J, Ponte J J, Alvarado F G, Mordan E, Amador J and Cascales C 1988 *Physica C* **156** 807
[5] Baraduc C, Pagnon V, Buzdin A, Henry J and Ayache C 1992 *Phys. Lett. A* **166** 267
[6] Malik S K and Shah S S 1992 *High Temperature Superconductivity* (NewYork: Nova Science)
[7] Loram W, Wheatley J M, Mirza K A and Liu R S 1992 *Phil. Mag. B* **65** 1405
[8] Ghosh A K, Bandyopadhyay S K, Barat P, Pintu S and Basu A N 1995 *Physica C* **255** 319
[9] Weaver B D, Jackson E M, Summers G P and Jackson E A 1992 *Phys. Rev. B* **46** 1134
[10] Anderson W and Zou Z 1988 *Phys. Rev. Lett* **60** 132
[11] Aslamazov L G and Larkin A I 1968 *Phys. Lett. A* **26** 238
[12] Lawrence W E, Doniach S and Proc S 1970 12*th International Conference of Low Tempature Physics* 1971 Keigaku, Tokyo, p. 361
[13] Gosh A K, Bandyopadhyay S K and Basu A N 1999 *J. Appl. Phys.* **86** 3247
[14] Ghosh A K, Bandyopadhyay S K, Barat P, PintuS and Basu A N 1996 *Physica C* **264** 255
[15] Ramallo M V, Torron C and Vidal F 1994 *Physica C* **230** 97
[16] Baraduc C and Bazdin A 1992 *Phys. Lett. A* **171** 408
[17] Ghosh A K, Bandyopadhyay S K, Barat P, PintuS and Basu A N 1995 *Physica C* **255** 319
[18] Reggiani L, Vaglio R and Varlamov A A 1991 *Phys. Rev. B* **44** 9541
[19] Vidal F, Veira J A, Maza J, Garcia-Alvarado F, Moran E and Alario M A 1988 *J. Phys. C* **21** L9
[20] Sedky A 2007 *J. Low Temp. Phys.* **148** 53
[21] Veira J A, Maza J and Vida F J 1988 *Phys. Lett. A* **131** 310
[22] Ghosh A K Bandyopadhyay S K and Basu A N 1997 *Mod. Phys. Lett. B* **11** 1013
[23] Ghosh A K and Basu A N 2000 *Supercond. Sci. Tech.* **13** 343
[24] Bhatia S N and Dhard C P 1994 *Phys. Rev. B* **49** 12206
[25] Rojas Sarmiento M P, Uribe Laverde M A, Vera Lopez E, Landinez Tellez D A and Roa Rojas J 2007 *Physica B* **398** 360
[26] Vovk R V, Obolenskii M A, Bondarenko A V, Goulatis I L and Chroneos A 2007 *Acta Phys. Pol.* **111** 129
[27] Presland M R, Tallon J L, Buckley R G, Liu R S and Floer N E 1991 *Physica C* **176** 95
[28] Matsuda A, Kinoshita K, Ishii T, Shibata H, Watanabe T and Yamada T 1988 *Phys. Rev. B* **38** 2910
[29] Mandal P, Poddar A and Das A N 1994 *J. Phys: Condens Matter* **6** 5689
[30] Ghorbani S R and Homaei M 2011 *Mod. Phys. Lett. B* **25** 1915
[31] Nawazish A K, Najmul H, Sana N, Babar S, Sajid K and Azhar A R 2010 *J. Appl. Phys.* **107** 083910
[32] Petrovie Y, Fasano R, Lortz M, Dcrous M, Potel M and Cheriel R 2007 *Physica C* **460** 702
[33] Gupta A , Lal R, Sedky A, Narlikar A V and Awana V P S 2001 *Phys. Rev. B* **61** 11752
[34] Wordenweber R , Heinemann K , Sastry G V S and Freyhardt H C 1989 *Physica C* **162** 1601
[35] Asaturian R A, Sarkissian A G, Ignatian E L and Begoian K G 1995 *Solid State Commun.* **95** 389
[36] Lobb C J 1987 *Phys. Rev. B* **36** 3930
[37] Loram J W, Copper J R and Mirza K A 1991 *Supercond. Sci. Tech.* **4** S391
[38] Cooper J R, Obretelli S D, Freeman P A and Zheng D N 1991 *Supercond. Sci. Tech.* **4** S277
[39] Rusiecki S, Bucher B, Kaldis E, Jilek E and Karpinski J 1990 *J. Less-Common Metals* **164** 31
[40] Ulm E R, Kim J T, Lemberger T R, Foltyn S R and Wu X 1995 *Phys. Rev. B* **51** 9193
[41] Porch A, Cooper J R, Zheng D N and Waldram J R 1993 *Physica C* **214** 350